

JPL D-19149

RADARSAT GEOPHYSICAL PROCESSOR SYSTEM

DATA USER'S HANDBOOK

(Version 2.0)

July, 2014

Ron Kwok
Glenn F. Cunningham

National Aeronautics and
Space Administration



Jet Propulsion Laboratory
California Institute of Technology
Pasadena, California

1.	INTRODUCTION.....	1
1.1	PURPOSE.....	1
1.2	DATA ARCHIVE/SOFTWARE	1
1.3	QUESTIONS.....	1
1.4	ACKNOWLEDGMENTS.....	2
1.5	RELATED DOCUMENTS.....	2
2.	MAP PROJECTION/GRIDDING	3
2.1	SSM/I POLAR STEREOGRAPHIC PROJECTION	3
2.2	GRID DEFINITION	3
2.3	GEOLOCATION ACCURACY	3
3.	RGPS OBSERVATIONS	5
3.1	REPEAT COVERAGE OF THE ARCTIC OCEAN	5
3.2	OBSERVATIONS DERIVED FROM THE IMAGE DATA.....	5
4.	PRODUCTS - TERMINOLOGY/ORGANIZATION	8
4.1	RGPS PROCESSING - GRID POINT AND CELL DATA	8
4.2	TEMPORAL COVERAGE OF PRODUCTS.....	8
4.3	PRODUCT FILE NAMING CONVENTION.....	8
5.	LAGRANGIAN ICE MOTION (PRODUCT L)	11
5.1	ALGORITHM OVERVIEW	11
5.2	DESCRIPTION (PRODUCT L) - LAGRANGIAN ICE MOTION	12
5.2.1	<i>Lagrangian Ice Motion: Metadata Record</i>	<i>12</i>
5.2.2	<i>Lagrangian Ice Motion: Image Description Data Records</i>	<i>12</i>
5.2.3	<i>Lagrangian Ice Motion: Gridpoint/Trajectory Description Data Records</i>	<i>12</i>
5.2.4	<i>Qflag Codes</i>	<i>14</i>
6.	BACKSCATTER HISTOGRAMS (PRODUCT B)	15
6.1	DESCRIPTION (PRODUCT B) - BACKSCATTER HISTOGRAMS.....	15
6.1.1	<i>Backscatter Histogram: Metadata Record</i>	<i>15</i>
6.1.2	<i>Backscatter Histograms: Backscatter range record.....</i>	<i>15</i>
6.1.3	<i>Backscatter Histograms: Histogram Data.....</i>	<i>15</i>
7.	ICE AGE/THICKNESS (PRODUCT T)	17
7.1	OVERVIEW OF ICE AGE ALGORITHM.....	17
7.1.1	<i>Age from Cell Area Changes</i>	<i>17</i>
7.1.2	<i>Age Distribution within a cell</i>	<i>18</i>
7.1.3	<i>Conversion of Ice Age to Ice Thickness</i>	<i>19</i>
7.1.4	<i>Thickness redistribution during ridging</i>	<i>19</i>
7.1.5	<i>Multiyear Ice Estimate</i>	<i>20</i>
7.2	DESCRIPTION (PRODUCT T) - ICE AGE/THICKNESS HISTOGRAMS	21
7.2.1	<i>Ice Age/Thickness Histograms: Metadata Record.....</i>	<i>21</i>
7.2.2	<i>Ice Age/Thickness Histograms: Interpolated Thickness Range Record</i>	<i>21</i>
7.2.3	<i>Ice Age/Thickness Histograms: Histogram Data</i>	<i>21</i>
8.	ICE DEFORMATION (PRODUCT D)	25
8.1	ALGORITHM OVERVIEW	25
8.2	DESCRIPTION (PRODUCT D) - ICE DEFORMATION	27
8.2.1	<i>Ice Deformation: Metadata Record</i>	<i>27</i>
8.2.2	<i>Ice Deformation: Area Change and Ice Motion Derivatives.....</i>	<i>27</i>

9.	AREA/OPEN WATER FRACTION (PRODUCT C)	29
9.1	ALGORITHM DESCRIPTION	29
9.2	DESCRIPTION (PRODUCT C) - OPEN WATER FRACTION	30
9.2.1	<i>Open Water Fraction: Metadata Record</i>	30
9.2.2	<i>Open Water Fraction: Area/Open Water Fraction Data</i>	30
10.	EULERIAN ICE MOTION (PRODUCT E)	31
10.1	DESCRIPTION (PRODUCT E) - EULERIAN ICE MOTION.....	31
10.1.1	<i>Eulerian Ice Motion: Metadata Record</i>	31
10.1.2	<i>Eulerian Ice motion: Motion Data</i>	31
11.	MELT ONSET /FREEZE UP (PRODUCT F)	33
11.1	ALGORITHM OVERVIEW	33
11.2	DESCRIPTION (PRODUCT F) - MELT ONSET/FREEZE UP	34
11.2.1	<i>Melt Onset/Freeze Up: Metadata Record</i>	34
11.2.2	<i>Melt Onset/Freeze Up: Dates</i>	34
12.	GRIDDED WIND/TEMPERATURE/PRESSURE FIELDS(PRODUCT M)	35
12.1	DESCRIPTION (PRODUCT M) - WIND/TEMPERATURE/PRESSURE FIELDS.....	36
12.1.1	<i>Gridded Wind/Temperature/Pressure: Metadata Record</i>	36
12.1.2	<i>Gridded Wind/Temperature/Pressure: Data</i>	36
13.	REFERENCES	37

Document Change Control

Release 1.0	Initial Release
Release 2.0	Corrected Qflag codes.

1. Introduction

The RADARSAT Geophysical Processor System (RGPS) produces Level 2 data products that contain descriptions of the Arctic Ocean sea ice cover derived from Synthetic Aperture Radar (SAR) imagery acquired by RADARSAT.

There are eight RGPS products containing the following derived information:

1. Lagrangian ice motion.
2. Backscatter histogram.
3. Ice age/Thickness histogram (winter only).
4. Ice deformation.
5. Area/open water fraction (summer only).
6. Eulerian ice motion.
7. Melt Onset/Freeze up.
8. Wind/Temp/Pressure Fields (50km grid).

Six products are produced directly from the Lagrangian ice motion record; they contain properties of material elements on the ice cover derived from their deformation and backscatter characteristics. The last product contains gridded sea level pressure, surface wind and temperature estimates used in the analysis of the SAR data.

1.1 Purpose

The purpose of this handbook is to provide the necessary information for the use of the data products generated by the RGPS. This includes an overview of the algorithms, description of the characteristics of the products and more importantly, brief descriptions of data fields in these products. The format and specifications of the actual products can be found in JPL Document D-13448.

1.2 Data Archive/Software

During the verification phase of the RGPS (between 1999-2000), all products are staged on the RGPS web site at JPL (URL: <http://www-radar.jpl.nasa.gov/rgps>). The RGPS product archive will be migrated to the Alaska SAR Facility at a future date. This web site also contains the latest information on RGPS processing plans and status. Software for reading the data products can be found there.

1.3 Questions

Questions can be directed to:

Ron Kwok
MS 300-331
Jet Propulsion Laboratory
4800 Oak Grove Dr
Pasadena, CA 91109

Phone: (818) 354-5614
FAX: (818) 393-3077
e-mail: ron.kwok@jpl.nasa.gov

1.4 Acknowledgments

This work was performed at the Jet Propulsion Laboratory, California Institute of Technology, under contract with the National Aeronautics and Space Administration.

1.5 Related Documents

Kwok, R., G. Cunningham and L. Nguyen, ASF RADARSAT Geophysical Processor System Product Specification, JPL D-13448.

Kwok, R. and G. F. Cunningham. ASF Geophysical Processor System Data User's Handbook, Version 2.0, JPL Document D-9526.

2. Map Projection/Gridding

The natural planimetric orientation of the image output of a strip map SAR processor is typically defined by the range and azimuth directions, where the azimuth direction is along the spacecraft groundtrack and the range direction (for a side-looking radar) is approximately orthogonal to that of the groundtrack. This is not the most convenient planimetric representation for geophysical analysis because of the inherent geometric characteristics and distortions. It does not allow for ease of registration of the data with SAR datasets collected with different imaging geometries and datasets acquired by other sensors. Furthermore, the projection characteristics (e.g. scale, orientation, etc.) are defined only within the extent of the image frame and therefore are not slowly varying and consistent for construction of large mosaics.

All the image data used in RGPS are geocoded. Geocoding is the process of resampling the image samples of a given planimetric representation, in this case the SAR range-azimuth projection, into one that is defined by a standard cartographic projection. The planimetric distortions of standard map projections are well-defined and slowly varying over large spatial scales. The process of geocoding involves the estimation of the geographic location (latitude, longitude) of each SAR image sample and then mapping it into the projection best-suited for a particular application. The polar stereographic projection used here is identical to the one used by the gridded Special Sensor Microwave/Imager (SSM/I) products. The rationale for this selection is that the RGPS products would be geometrically registered to the gridded SSM/I products without resampling of the data fields.

2.1 SSM/I Polar Stereographic Projection

The reference latitude of the SSM/I polar stereographic projection is located at 70°N. The decision to lower the tangent plane from the pole to the 70° latitude was made to minimize geometric distortions in the marginal ice zone. The origin of the Cartesian grid is at the North pole. The map vertical (or the ordinate) and the abscissa of the grid are defined by the 135°E and 45°E meridians. Planimetrically, this is a conformal projection with true scale at the reference latitude. The scale is 0.97 at the pole. The Hughes ellipsoid is used as the projection datum. Details of the SSM/I polar grids can be found in [DMSP, 1996].

2.2 Grid Definition

There are four grid sizes defined by the original SSM/I polar grids. For both polar regions, a 100km grid cell is centered at the pole. The 12.5 km, 25 km, 50 km and 100 km grids all share the same outer boundary with the smaller grid cells being partitions of the 100km grid. For example, there are four 50km grid cells within every 100km grid cell. A 5 km and 10 km grid have been added to the polar grids to allow for the higher resolution sampling required by the RGPS products.

2.3 Geolocation Accuracy

Many factors affect the absolute geolocation of a grid point. By far, the dominant source of error in the location of an image pixel is the uncertainty in the ephemeris of the

RADARSAT platform. The Canadian Space Agency (CSA) provides the Alaska SAR Facility with restituted state vectors after reception of a data take for image product generation. These state vectors have location accuracies better than that of the orbit predicts. Based on comparison of the estimated location of corner reflectors in a SAR image and the location of these reflectors (measured with hand held GPS receivers), the location uncertainty of the products generated at ASF is typically 100m for descending passes and 200m for ascending passes. Also, it was found that these errors are highly correlated between ascending passes and between descending passes. The random component of these errors is approximately 50 m and includes uncertainty introduced in the measurement process. The pixel location accuracy quoted here is based on preliminary evaluation of the commissioning phase data. There is continuing effort to characterize and improve this quantity in future image products.

3. RGPS Observations

3.1 Repeat Coverage of the Arctic Ocean

The 460 km swath ScanSAR Wide B (SWB) mode of RADARSAT [Raney et al, 1992] is selected to provide routine coverage of the Arctic Ocean for the RGPS system. The radar data are downlinked in real-time while the satellite is within line-of-sight of the ASF or Tromso reception stations. Outside the two station masks, the radar data are acquired and stored on the onboard tape recorder (OBR) and downlinked to Canadian ground stations at a later time. The planned coverage of the Arctic Ocean over a 24-day *cycle* (the number of days it takes for the spacecraft to retrace the same orbit) is shown in Fig. 1. The Arctic Ocean within the ASF mask is covered once every three days and within the Tromso mask once every six days.

3.2 Observations derived from the Image Data

The direct measurements from sequential RADARSAT ScanSAR Wide B (SWB) imagery are sea ice motion and backscatter. The ice age and ice thickness estimates are derived from the record of ice motion and deformation. The measurements made at each time step are stored in three database tables maintained in the RGPS system (Table 1). These tables are: the grid point trajectory table, connectivity table and the cell attributes table.

Grid point trajectory Table. At each time step, the geographic location of a grid point is recorded. Birth date is the date that grid point was created. When that grid point is deleted, the death date is recorded. This table is updated each time a grid point is tracked to a new location. Displacement vectors are computed from differences in their geographic locations.

Connectivity Table. We keep track of the number of points of a polygon used to define a *cell* in this table. For each cell, the unique grid point identifiers of each vertex of the polygon are stored. Birth date is the date the cell was created. Initially, a cell is defined by a polygon with four vertices. Grid points are added as the length of the sides of the polygon increases. The connectivity table is updated when a grid point or cell is added or deleted. For example, when a grid point is deleted, the cells that are defined by that grid point are no longer valid and thus cause the death of the cells associated with this grid point. A grid point is deleted when the point is advected out of the region of interest or that point could no longer be identified by the ice tracker.

Cell Attributes Table. The attributes of each cell (e.g. backscatter histogram, multiyear ice fraction, area, etc.) at each time step are stored in this table. These attributes are listed in Table 1.

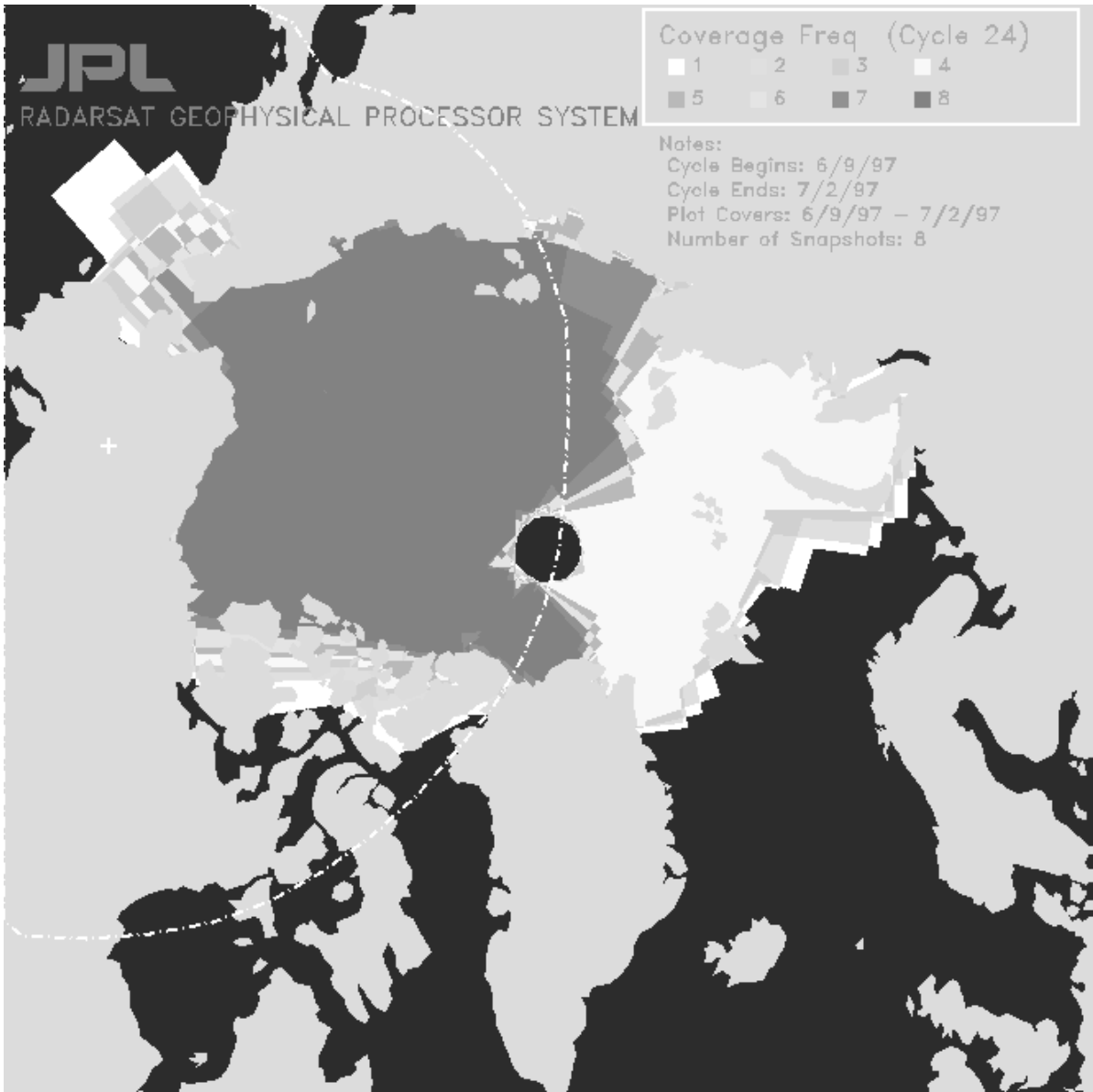


Fig 1. Nominal repeat coverage of the Arctic Ocean over a 24-day cycle.

Table 1

RGPS Database Tables

<i>Grid Point Trajectories</i>	
Grid Point identifier 1	Time of Observation Latitude Longitude Birth Date Death Date
Grid Point identifier 2	Time of Observation
:	:
<i>Grid Connectivity Table</i>	
Cell identifier 1	Number of Vertices (N) Grid point identifier 1 : Grid point identifier N Birth Date Death Date
Cell identifier 2	Number of Vertices (N)
:	:
<i>Cell Attributes Table</i>	
Cell identifier 1	Time of observation Area Air Temperature Wind u,v Winter: multiyear ice area Summer: open water fraction Incidence angle Backscatter histogram
Cell identifier 2	Time of observation
:	:

4. Products - Terminology/Organization

4.1 RGPS Processing - Grid Point and Cell Data

We process one n-day snapshot of the Arctic Ocean at a time. An n-day *snapshot* is the number of days it takes to cover a selected region using a collection of datatakes. Nominally, n=3 for repeat coverage in the ASF mask and n=6 for repeat coverage outside the mask.

Sequential image data from the n-day snapshots are processed as separate streams. A *stream* contains the trajectories of all grid points and time-varying cell attribute information defined on the image frames of an initial datatake. Fig. 2 shows an initial sample grid of a stream. The image frames of the first datatake in a sequence define the spatial coverage of the initial grid of that particular stream. No grid points are created automatically after the first grid is established. Ice motion of these points and cell attributes are sampled in subsequent n-day snapshots. Each stream is processed independently of one another.

Grids with two different spacings are established in each stream to sample the ice motion and cell attributes. A 25 km coastal grid covers the region between the land boundaries and 100 km off the coast. A finer grid, either 10 km or 20 km, is used to sample ice motion away from the coast.

The products and their temporal and spatial sampling characteristics are shown in Table 2.

4.2 Temporal Coverage of Products

We produce products L (Lagrangian ice motion), B (backscatter), T (age/thickness), D (deformation), C (area/open water fraction) and M (wind/temp/pressure) in Table 2 at the end of every month of observations of the Arctic Ocean. Products L and D contain all observations of gridpoints or cells from the initial datatake through the end of the month. Products, B, T and C contain only those observations made within the product's month. Product F (melt onset/freeze-up) is produced only twice a year. Product E (Eulerian ice motion) contains the ice motion field derived from two sequential images sampled on a 5-km uniformly-spaced grid.

4.3 Product file naming convention

File Name: PnpppSYDddd.TF

where

Pn: Platform and number ("R1")
ppp: Product ID (1-999)
S: Data stream ID (a-z, A-Z)
YY: Start year of the product

DDD: Start julian day of the product
 ddd: Duration (in days) that the product spans
 T: Product code, according to the code described in Table 2
 F: File type (“P” for product, “M” for metadata)

Table 2

RGPS Data Products

(The initial spacing of the Lagrangian grids are either 10 km or 20 km)

Product Code	Description	Season	Grid Spacing	Temporal Samping (nominal)
L	Lagrangian motion trajectories	Winter/Summer	Variable	3-6 days
B	Backscatter histogram	Winter/Summer	Variable	3-6 days
T	Ice age/thickness histogram	Winter	Variable	3-6 days
D	Ice deformation	Winter/summer	Variable	3-6 days
C	Area/open water fraction	Summer	Variable	3-6 days
E	Eulerian ice motion	Winter/Summer	5, 10 km	N/A
F	Melt Onset/Freeze Up	Winter/Summer	Variable	3-6 days
M	Wind/Temp/Pressure Fields	Winter/Summer	50 km	Daily

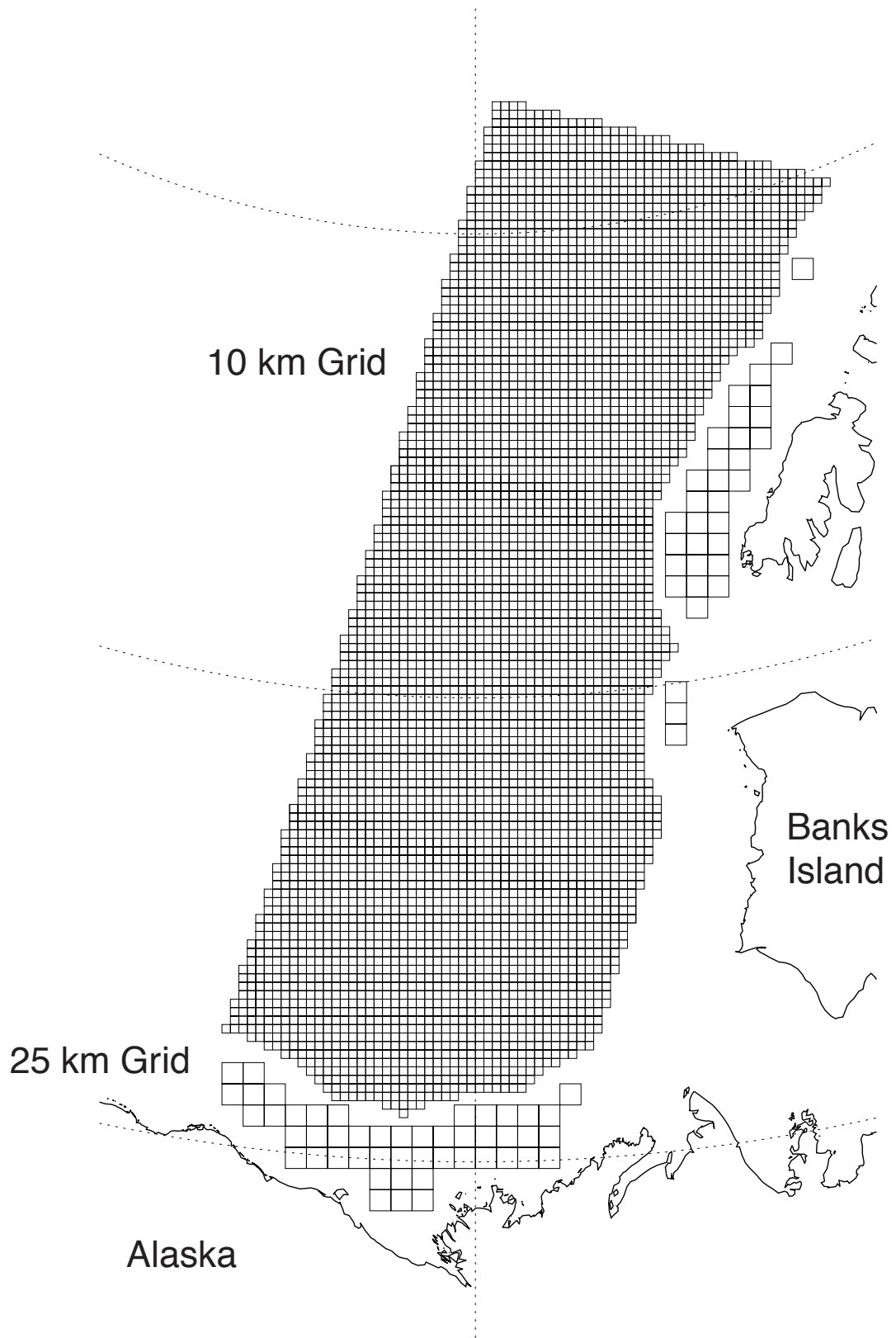


Fig. 2 Example of an initial grid overlaid on a ScanSAR datatake at the beginning of a stream.

5. Lagrangian Ice Motion (Product L)

5.1 Algorithm Overview

The ice motion tracker is based on the procedure described in *Kwok et al. (1990)*. The ice tracking algorithm operates on pairs of images separated in time. It uses area matching techniques to follow an array of points (defined as the center of an area on an image) from a source image to a set of target images. The time separation between repeat observations is variable and is based on available coverage. Initially, a regular array of points is defined on the first set of images covering a region. The common ice features are identified in sequential image frames by the ice tracker. Each point acquires its own trajectory as these points move with the ice cover. This differs from the ERS-1 GPS ice tracking strategy, in which the motion between image pairs are referred to an Earth-fixed grid, giving a quasi-Eulerian picture of the displacement field. Here, the RGPS uses the ice tracker to follow the same set of points over an ice season, giving a densely sampled Lagrangian picture of ice motion identical to the trajectories derived from drifting buoys.

5.2 Description (Product L) - Lagrangian Ice Motion

This product contains the trajectories of all the grid points within a stream over a time interval between *PRODUCT_START_YEAR/TIME* and *PRODUCT_END_YEAR/TIME*. This product is produced on a monthly basis.

5.2.1 Lagrangian Ice Motion: Metadata Record

Field Name	Description
<i>PID</i>	RGPS product identifier (see section 4).
<i>PROD_DESCRIPTION</i>	Description of Product e.g. Lagrangian Ice Motion, Deformation, etc.
<i>N_IMAGES</i>	Number of images used in the creation of this product.
<i>N_TRAJECTORIES</i>	Number of trajectories contained in this product.
<i>PROD_TYPE</i>	'Winter' or 'Summer' Product
<i>CREATE_YEAR</i> , <i>CREATE_TIME</i>	The year/time this product was created by the RGPS system.
<i>PRODUCT_START_YEAR</i> , <i>PRODUCT_START_TIME</i>	The year/time limit for the earliest observation.
<i>PRODUCT_END_YEAR</i> , <i>PRODUCT_END_TIME</i>	The year/time limit for the latest observation.
<i>SW_VERSION</i>	The version of the RGPS software used to create this product.
<i>NW_LAT</i> , <i>NW_LONG</i> , <i>NE_LAT</i> , <i>NE_LONG</i> , <i>SW_LAT</i> , <i>SW_LONG</i> , <i>SE_LAT</i> , <i>SE_LONG</i>	The corner points of the initial datatake. The initial gridpoints are created within these bounds.

5.2.2 Lagrangian Ice Motion: Image Description Data Records

The image description data contain one record for each image used in the construction of the ice motion trajectories. All the images used in the creation of this product are stored here. This can be used to locate a grid point on a particular image.

Field Name	Description
<i>IMAGE_ID</i>	ASF image identifier.
<i>IMAGE_YEAR</i> , <i>IMAGE_TIME</i>	Time/year of image center.
<i>MAP_X</i> , <i>MAP_Y</i>	The map location of the image center.

5.2.3 Lagrangian Ice Motion: Gridpoint/Trajectory Description Data Records

The gridpoint description data contain one record for each gridpoint and its trajectory.

Field Name	Description
<i>GPID</i>	Unique gridpoint identifier assigned when the grid is defined on the initial datatake.
<i>BIRTH_YEAR,</i> <i>BIRTH_TIME</i>	The year/time of this gridpoint's first observation.
<i>DEATH_YEAR</i> <i>DEATH_TIME</i>	The year/time when this gridpoint was deleted. A grid point is deleted when it could no longer be tracked by the motion tracker. This terminates the trajectory of this grid point but the available observations remain in the product.
<i>N_OBS</i>	This number of observations of this gridpoint in this product.
<i>OBS_YEAR_1,</i> <i>OBS_TIME_1</i>	The year/time of the first observation.
<i>X_MAP_1,</i> <i>Y_MAP_1</i>	The map location of the gridpoint during this observation.
<i>Q_FLAG_1</i>	<p>Quality flag (I_m)- an output of the tracker. Lower values indicate that the confidence of the matches are high.</p> <p>ρ = correlation peak of the image patches. m, σ = mean and standard deviation of all the matches between two images. (values > 6 describe history of the grid point – see explanation in following pages)</p> <p> $I_m=1$ if $m < \rho$; $I_m=2$ if $m - 0.5\sigma < \rho < m$; $I_m=3$ if $m - \sigma < \rho < m - 0.5\sigma$; $I_m=4$ if $m - 1.5\sigma < \rho < m - \sigma$; $I_m=5$ if $m - 2.0\sigma < \rho < m - 1.5\sigma$; $I_m=6$ if $m - 2.5\sigma < \rho < m - 2.0\sigma$. </p>
.	.
.	.
.	.
<i>OBS_YEAR_N,</i> <i>OBS_TIME_N</i>	The year/time of the <i>N</i> th observation.
<i>X_MAP_N,</i> <i>Y_MAP_N</i>	The location of the grid point during this observation.
<i>Q_FLAG_N</i>	Quality flag - an output of the tracker.

5.2.4 Qflag Codes

The sequence of modifications to the location of a gridpoint during an inspection session are recorded in the *Qflag* codes:

(Notes: During an inspection session, the operator has the option to define an area to send to ice motion tracking procedure (sub-tracker) for refinement of the grid point positions.)

Code	Description
	1 : Unchanged with initial tracker quality 1 [tq1]
	2 : Unchanged with initial tracker quality 2 [tq2]
	3 : Unchanged with initial tracker quality 3 [tq3]
	4 : Unchanged with initial tracker quality 4 [tq4]
	5 : Unchanged with initial tracker quality 5 [tq5]
	6 : Unchanged with initial tracker quality 6 [tq6]
	-235 : Manipulated by operator manually or using a subtracker

6. Backscatter Histograms (Product B)

6.1 Description (Product B) - Backscatter Histograms

This product contains the backscatter histograms of pixel samples within each cell.

6.1.1 Backscatter Histogram: Metadata Record

Field Name	Description
<i>PID</i>	RGPS product identifier (see section 4).
<i>PROD_DESCRIPTION</i>	Description of Product e.g. Lagrangian Ice Motion, Deformation, etc.
<i>N_CELLS</i>	Number of cells in this product.
<i>PROD_TYPE</i>	'Winter' or 'Summer' Product
<i>CREATE_YEAR,</i> <i>CREATE_TIME</i>	The year/time this product was created by the RGPS system.
<i>PRODUCT_START_YEAR,</i> <i>PRODUCT_START_TIME</i>	The year/time limit for the earliest observation.
<i>PRODUCT_END_YEAR,</i> <i>PRODUCT_END_TIME</i>	The year/time limit for the latest observation.
<i>SW_VERSION</i>	The version of the RGPS software used to create this product.
<i>NW_LAT, NW_LONG,</i> <i>NE_LAT, NE_LONG,</i> <i>SW_LAT, SW_LONG,</i> <i>SE_LAT, SE_LONG</i>	The corner points of the initial datatake. The initial gridpoints are created within these bounds.

6.1.2 Backscatter Histograms: Backscatter range record

The backscatter range record describes the backscatter range of each category in the backscatter histogram.

Field	Description
<i>BSR_1, BSR_2, ...BSR_25</i>	Backscatter range within each category

6.1.3 Backscatter Histograms: Histogram Data

The histograms are stored here.

Field Name	Description
<i>CELL_ID</i>	Cell identifier
<i>BIRTH_YEAR,</i> <i>BIRTH_TIME</i>	The year/time this cell was created.
<i>I_AREA</i>	Initial cell area.
<i>N_OBS</i>	Number of observations of this cell.
<i>OBS_YEAR_1,</i>	The year/time of the first observation.

<i>OBS_TIME_1</i>	
<i>X_MAP_1</i> , <i>Y_MAP_1</i>	The center location of this cell.
<i>C_TEMP_1</i>	2-m air temperature at cell center.
<i>C_AREA_1</i>	Current cell area.
<i>MYFRAC_1</i>	Multiyear ice fraction.
<i>OWFRAC_1</i>	Open water fraction.
<i>FBSR_1... FBSR_25</i>	Fractional area in each backscatter range category.
<i>INC_ANG_1</i>	Incidence angle at cell center.
<i>OBS_YEAR_N</i> , <i>OBS_TIME_1</i>	The year/time of (N_OBS) observation.
<i>X_MAP_N</i> , <i>Y_MAP_N</i>	The center location of (N_OBS) cell.
<i>C_TEMP_N</i>	2-m air temperature at (N_OBS) cell center.
<i>C_AREA_N</i>	(N_OBS) cell area.
<i>MYFRAC_N</i>	Multiyear ice fraction of (N_OBS) cell.
<i>OWFRAC_N</i>	Open water fraction of (N_OBS) cell.
<i>FBSR_1... FBSR_25</i>	Fractional area in each backscatter range category.
<i>INC_ANG_N</i>	Incidence angle at (N_OBS) cell center.

7. Ice Age/Thickness (Product T)

7.1 Overview of Ice Age Algorithm

The ice age distribution specifies the fractional area covered by ice in different age categories at a given time. We note here that the algorithm works only during the winter months (ice growth season) and that the procedure resolves the age categories at the young end of the distribution [Kwok *et al.*, 1995]. Here, we describe how we associate cell area changes to ice age. A *cell* is the area within an image defined by the straight-line segments connecting n grid points. Then, we discuss a computational procedure to determine the age distribution of ice within a cell. We want to estimate the areal contribution $B_{k,j}$ of each age category j at time t_k to the total observed area. The age resolution is dependent on the frequency of observation of a given cell. The sampling interval between observations does not have to be constant.

7.1.1 Age from Cell Area Changes

In the ice age algorithm, we monitor the time series of area changes of the cells. An increase in area indicates that new ice was formed in the cell. A negative change is assumed to have ridged the youngest ice in the cell, reducing its area. The assumption here is that once ridging starts, the deformation tends to be localized in the thinner, weaker ice that recently formed in the lead systems. The age classes are determined by the lengths of the time steps. The multiyear ice area within the cell is estimated from the backscatter histogram from within the cell. These data are recorded and tabulated. Each record applies to the time of one scene and records the change since the last observation. These are the fundamental data for computing the age distribution. The age distribution, $B_{k,j}$ is a set of areas of different age classes. $B_{k,j}$ denotes the area of ice at time t_k of age category j . That is, the age of the ice satisfies the inequalities

$$t_k - t_{k-(j-1)} < age_{k,j} < t_k - t_{k-j} \text{ for } j = 2 \text{ to } k-1 .$$

Actual numerical examples can be found in [Kwok *et al.*, 1995]. The index k denotes time t_k ; the index j denotes age class, increasing with age class. T_k denotes the mean temperature during the time interval $[t_k, t_{k-1}]$; A_k is the area of the cell at time t_k .

The quantity $B_{k,MY}$ is the area of multiyear (MY) ice in the cell at time t_k , as determined from the backscatter within the cell. We use the ice classification algorithm in the GPS for this purpose. Theoretically this should not depend on k (time) because no MY ice should be created in the winter, but errors in the classification of multiyear ice can result from wind-blown open water or frost flowers. These confounding effects can be identified and removed by considering the time series of the multiyear ice area: $B_{1,MY}$, $B_{2,MY}, \dots, B_{k,MY}$. This filtering problem is discussed later. The quantity $B_{k,FY}$ is the area of ice in the cell at time t_k older than $t_k - t_1$ but younger than multiyear ice, i.e. it is the older first-year (FY) ice. The oldest ice (other than FY and MY) which is observed in this procedure is dependent on the length of time required to 'integrate' out the initial conditions (discussed in Section 4). At time t_1 , the area $B_{1,MY}$ is computed from the backscatter within the cell.

7.1.2 Age Distribution within a cell

Suppose that the complete age histogram is known at time t_{k-1}

$$B_{k-1,1}, B_{k-1,2}, \dots, B_{k-1,k-2}, B_{k-1,FY}, B_{k-1,MY}$$

The computational procedure to obtain the histogram $B_{k,j}$ at time t_k is as follows:

1) The first step is a shift of the histogram that represents the aging process.

$$B_{k,j} \leftarrow B_{k-1,j-1} \text{ for } j=2 \text{ to } k-1$$

For example, the first equation $B_{k,2} \leftarrow B_{k-1,1}$ says that the area of ice at time t_{k-1} (which was older than 0 but younger than $t_{k-1} - t_{k-2}$) is transferred into the class of ice that is older than $t_k - t_{k-1}$ but younger than $t_{k-1} - t_{k-2}$. In other words, we have added $\Delta t = t_k - t_{k-1}$ to the upper and lower bounds of the age class. A similar interpretation applies to the other equations. Note that $B_{k,1}$ is not defined yet. It is determined in the next step.

2) Compute the new total cell area, A_k , from the new positions of the grid points. Compute the change in cell area since the previous time: $\Delta A = A_k - A_{k-1}$. The area of the youngest ice class is now $B_{k,1} = \max(0, \Delta A)$. In other words, if new area was created ($\Delta A > 0$) then set the area of the youngest class to ΔA . If area was lost ($\Delta A < 0$) then set the area of the youngest class to zero. Step 4 accounts for any loss in area.

3) If $\Delta A \geq 0$ then skip to step 5.

4) This step is only executed when the cell area decreases ($\Delta A < 0$). We need to remove the area ΔA from the histogram. We first remove area from the next class $B_{k,2}$ and then older classes, as necessary, until a total area reduction of ΔA is achieved. The assumption is that we are ridging the youngest ice first. The ridging process is fully described later on in this section.

5) The area of multiyear ice $B_{k,MY}$ is computed from the backscatter within the cell using the GPS ice classification algorithm [Kwok *et al.*, 1992].

6) Although we do not provide an estimate of $B_{k,FY}$, it can be estimated as follows:

$$B_{k,FY} = A_k - [B_{k,1} + B_{k,2} + \dots + B_{k,k-1} + B_{k,MY}]$$

Since $B_{k,MY}$ is an independent estimate, it is possible that the area of first-year ice computed could be less than 0.

This completes the determination of the areas $B_{k,j}$ at time t_k . The procedure is repeated whenever Lagrangian observations of grid points are available. We refer to the time interval between sequential images as a time step. During each time step, the cell areas

are computed. The area of ice in each age class in each cell is updated at each time step. In this manner, we keep track of the age distribution of the young ice within every cell.

7.1.3 Conversion of Ice Age to Ice Thickness

To convert age to ice thickness, we must know the freezing rate. We approximate this rate as being proportional to the number of freezing-degree days (FDD) associated with each age class of each cell. We convert the age distribution to thickness distribution with a simple procedure which utilizes the dependence of thickness, H , on freezing-degree days, F . For each category of young ice, there are upper and lower bounds on the age of the ice due to the length of each time step: the opening in the ice could be created during the beginning or near the end of the time step. Consequently there are two values of F , upper and lower bounds, that apply to each age category. We do not keep track of F for the first-year and multiyear classes. We used Lebedev's parameterization (discussed in *Maykut*, 1986), with $H = 1.33 F^{0.58}$. This relationship is based on 24 station years of observations from various locations in the Soviet Arctic. Lebedev's parameterization describes ice growth under "average" snow conditions, in contrast to others which describes ice growth with little or no snow cover. The thickness of the snow cover is an important parameter which controls ice growth, but there is at present no routine measurements of snow depth over the ice cover which could be used for better estimation of the growth rate.

The high rate of ice growth when the ice is young gives the largest uncertainty in the thickness in this youngest age class. This relative uncertainty improves as the ice ages and the growth rate decreases.

7.1.4 Thickness redistribution during ridging

The ridging process is dependent on the parameter that describes the ratio (k) of the thickness of an ice ridge to the thickness of the ice being ridged. Here, we set $k = 5$ [*Parmeter and Coon*, 1972] for ice with thickness $> 80\text{cm}$ and $k = 2$ for ice $\leq 80\text{cm}$. The ridging process uses these k ratios so that ice volume is conserved in the process.

In the procedure, three types of ice are available for ridging: (1) young ice that has been created since the birth of the cell, (2) rafted or ridged young ice, and (3) ice present at the time of cell creation. When a cell decreases in area (i.e. ice is being ridged or rafted), the freezing-degree-days values of ice types (1) and (2) within the cell are examined. Ridged ice is given an equivalent freezing-degree-days value calculated from its thickness. The ice with the minimum FDD value is ridged first, using the appropriate k value as described above. The procedure continues until the necessary area change is attained. The ridge continues to grow as it accumulates freezing-degree-days. When ridging is required and there are no type (1) or (2) ice within a cell, type (3) ice is ridged into the "FY-ridged" category. This category does not contain any ridge thickness information.

As described in the previous section, ridging only occurs when a cell undergoes a decrease in area, ΔA . Let us define the area to be removed as A_r . Initially, $A_r = \Delta A$. A_i , the area of type i ice, is ridged first. The area available for ridging is:

$$A_{avail} = A_i * (k-1) / k$$

since as soon as this much ice is ridged, the newly ridged ice is “piled” onto the remaining unridged ice within that area.

If $A_r < A_{avail}$, a single ridge is formed with thickness h_{R_i} with areal coverage A_{R_i} of:

$$h_{R_i} = h_i k, \quad A_{R_i} = A_r / (k-1)$$

where h_i is the thickness of the ice that was ridged. The remaining area of the chosen ice category is updated to:

$$A_{i_{new}} = A_i - A_r - A_{R_i}$$

Since $A_{R_i} h_{R_i} + A_{i_{new}} h_i = A_i h_i$, the total ice volume is conserved.

If $A_r \geq A_{avail}$, a ridge is formed with thickness h_{R_i} and covers an area A_{R_i} where,

$$h_{R_i} = h_i k, \quad A_{R_i} = A_i / k$$

The area of the chosen ice category that was ridged is then set to zero. The area that must still be removed is updated to $A_r = A_r - A_{avail}$. The next ice category is chosen and the procedure repeats until $A_r = 0$. In the case of ice type (3) being ridged, the ridge area is $A_{R_i} = A_r / (k-1)$.

7.1.5 Multiyear Ice Estimate

A simple backscatter based classifier [Kwok *et al.*, 1992] is used to determine the multi-year ice area within each cell.

7.2 Description (Product T) - Ice Age/Thickness Histograms

This product contains the ice age/thickness histograms of all the cells in the database at the time this product was produced. The ice age/thickness categories do not have uniform age intervals.

7.2.1 Ice Age/Thickness Histograms: Metadata Record

Field Name	Description
<i>PID</i>	RGPS product identifier (see section 4).
<i>PROD_DESCRIPTION</i>	Description of Product e.g. Lagrangian Ice Motion, Deformation, etc.
<i>N_CELLS</i>	Number of cells used in the creation of this product.
<i>CREATE_YEAR</i> <i>CREATE_TIME</i>	The year/time this product was created by the RGPS system.
<i>PRODUCT_START_YEAR</i> <i>PRODUCT_START_TIME</i>	The year/time limit for the earliest observation.
<i>PRODUCT_END_YEAR</i> <i>PRODUCT_END_TIME</i>	The year/time limit for the latest observation.
<i>SW_VERSION</i>	The version of the RGPS software used to create this product.
<i>NW_LAT, NW_LONG</i> <i>NE_LAT, NE_LONG</i> <i>SW_LAT, SW_LONG</i> <i>SE_LAT, SE_LONG</i>	The corner points of the initial data area. The initial gridpoints are created within these bounds.

7.2.2 Ice Age/Thickness Histograms: Interpolated Thickness Range Record

The interpolated thickness range record describes the thickness interval of each thickness category.

Field Name	Description
<i>THICK_STEP</i>	The range of each thickness category

7.2.3 Ice Age/Thickness Histograms: Histogram Data

The histogram data contain one record per cell observed. The records are in row order. Each record has the following format.

Field Name	Description
<i>CELL_ID</i>	Unique cell identifier.
<i>BIRTH_YEAR</i> , <i>BIRTH_TIME</i>	The year/time this cell was created.
<i>I_AREA</i>	Initial cell area.
<i>N_OBS</i>	Number of observations of cell.
<i>OBS_YEAR_1</i> , <i>OBS_TIME_1</i>	The year/time of this observation.
<i>X_MAP_1</i> , <i>Y_MAP_1</i>	The center location of this cell.
<i>C_TEMP_1</i>	Air temperature at cell center.
<i>FDD_1</i>	Accumulated freezing degree days since cell creation.
<i>C_AREA_1</i>	Current cell area.
<i>N_AGE_1</i>	Number of age categories up to and including the oldest observation.
<i>AR_1_1</i>	Age range (youngest ice) of first category.
<i>AGE_FAR_1_1</i>	Fractional area in 1st age range.
<i>FDD_1_1</i>	Accumulated freezing degree days of 1st age range.
.	.
.	.
.	.
<i>AR_N_1</i>	Age range of category (<i>N_AGE_1</i>)
<i>AGE_FAR_N_1</i>	Fractional area within (<i>N_AGE_1</i>) age range
<i>FDD_N_1</i>	Accumulated freezing degree days of (<i>N_AGE_1</i>) age range
<i>N_THICK_1</i>	Number of thickness categories up to and including the thickest observation
<i>THICK_FAR_1_1</i>	Fractional area in 1 st thickness range
.	.
.	.
.	.
<i>THICK_FAR_N_1</i>	Fractional area in (<i>N_THICK</i>) thickness range
<i>FAR_FYR_1</i>	Fractional area within ridged-FY category
<i>FAR_MY_1</i>	Fractional area in radiometric MY category
<i>N_RIDGE_1</i>	Number of ridging event records
<i>RIDGE_AR_1_1</i>	Age range of ice in ridging event 1
<i>RIDGE_FAR_1_1</i>	Fractional area of ice in ridging event 1
<i>RIDGE_FDD_1_1</i>	Accumulated freezing degree days of ice in ridging event 1
<i>RIDGE_FLAG_1_1</i>	<i>0 = old ridge, 1 = new ridge</i> A new ridge is one formed during this time step. An old ridge is one formed at a previous time step.
.	.
.	.
.	.

<i>RIDGE_AR_N_I</i>	Age range of ice in ridging event N_RIDGE
<i>RIDGE_FAR_N_I</i>	Fractional area of ice in ridging event N_RIDGE
<i>RIDGE_FDD_N_I</i>	Accumulated freezing degree days of ice in ridging event N_RIDGE
<i>RIDGE_FLAG_N_I</i>	<i>0 = old ridge, 1 = new ridge</i>
.	.
.	.
.	.
<i>OBS_YEAR_N,</i> <i>OBS_TIME_N</i>	The year/time of this observation.
<i>X_MAP_N,</i> <i>Y_MAP_N</i>	The center location of this cell.
<i>C_TEMP_N</i>	Air temperature at cell center.
<i>FDD_N</i>	Accumulated freezing degree days since cell creation.
<i>C_AREA_N</i>	Current cell area.
<i>N_AGE_N</i>	Number of age categories up to and including the oldest observation.
<i>AR_1_N</i>	Age range (youngest ice) of first category.
<i>AGE_FAR_1_N</i>	Fractional area in 1st age range.
<i>FDD_1_N</i>	Accumulated freezing degree days of 1st age range.
.	.
.	.
.	.
<i>AR_N_N</i>	Age range of category (N_AGE_1)
<i>AGE_FAR_N_N</i>	Fractional area within (N_AGE_1) age range
<i>FDD_N_N</i>	Accumulated freezing degree days of (N_AGE_1) age range
<i>N_THICK_N</i>	Number of thickness categories up to and including the thickest observation
<i>THICK_FAR_1_N</i>	Fractional area in 1 st thickness range
.	.
.	.
.	.
<i>THICK_FAR_N_1</i>	Fractional area in (N_THICK) thickness range
<i>FAR_FYR_N</i>	Fractional area within ridged-FY category
<i>FAR_MY_N</i>	Fractional area in radiometric MY category
<i>N_RIDGE_N</i>	Number of ridging event records
<i>RIDGE_AR_1_N</i>	Age range of ice in ridging event 1
<i>RIDGE_FAR_1_N</i>	Fractional area of ice in ridging event 1
<i>RIDGE_FDD_1_N</i>	Accumulated freezing degree days of ice in ridging event 1
<i>RIDGE_FLAG_1_N</i>	<i>0 = old ridge, 1 = new ridge</i> A new ridge is one formed during this time step. An old ridge is one formed at a previous time step.
.	.

.	.
<i>RIDGE_AR N N</i>	Age range of ice in ridging event N_RIDGE
<i>RIDGE_FAR N N</i>	Fractional area of ice in ridging event N_RIDGE
<i>RIDGE_FDD N N</i>	Accumulated freezing degree days of ice in ridging event N_RIDGE
<i>RIDGE_FLAG N N</i>	<i>0 = old ridge, 1 = new ridge</i>

8. Ice Deformation (Product D)

This product contains cell area changes and spatial derivatives computed using ice displacements at the cell vertices.

8.1 Algorithm Overview

The displacement gradients are calculated as follows. The Divergence Theorem in two dimensions states that

$$\iint \left[\frac{\partial P}{\partial x} + \frac{\partial Q}{\partial y} \right] dx dy = \oint [P dy - Q dx] \quad (1)$$

Where the double integral on the left is taken over a region of area A , and the contour integral on the right is taken around the boundary of that region. Define the area-averaged value of some quantity $R(x,y)$ as

$$\bar{R} = \frac{1}{A} \iint R(x,y) dx dy \quad (2)$$

With $P = u$ and $Q = 0$ in (1), and letting u_x denote the area-averaged value of $\partial u / \partial x$, equation (1) becomes

$$u_x = \frac{1}{A} \oint u dy \quad (3)$$

Analogous definitions for the other partial derivatives are as follows:

$$u_y = -\frac{1}{A} \oint u dx \quad v_x = \frac{1}{A} \oint v dy \quad v_y = -\frac{1}{A} \oint v dx \quad (4)$$

The integrals in equations (3) and (4) are approximated using the known positions and displacements of the vertices of the cell. Let (x, y) be the vertices (in counter-clockwise order) at the time prior to the current observation, and let (u, v) be the displacements of those vertices over the ensuing time interval (DELTA_TIME). Then the integral in equation (3) is approximated as

$$u_x = \frac{1}{A} \sum_{i=1}^n \frac{1}{2} (u_{i+1} + u_i) (y_{i+1} - y_i) \quad (5)$$

Where n is the number of vertices, and the subscripts are cyclical (e.g. $u_{n+1} = u_1$). This results from the trapezoid integration rule, in which $u(x,y)$ is approximated as a linear

function between points I and $I+1$. Analogous formulas can be written down for the other partial derivatives. Incidentally, the area A is given by

$$A = \frac{1}{2} \sum_{i=1}^n (x_i y_{i+1} - y_i x_{i+1})$$

(6)

This follows from equation (1) with $P=x$ and $Q=y$.

8.2 Description (Product D) - Ice Deformation

This product contains cell area changes and spatial derivatives computed using ice displacements at the cell vertices.

8.2.1 Ice Deformation: Metadata Record

Field Name	Description
<i>PID</i>	RGPS product identifier (see section 4).
<i>PROD_DESCRIPTION</i>	Description of Product e.g. Lagrangian Ice Motion, Deformation etc.
<i>N CELLS</i>	Number of cells contained in this product.
<i>PROD_TYPE</i>	'Winter' or 'Summer' Product
<i>CREATE_YEAR,</i> <i>CREATE_TIME</i>	The year/time this product was created by the RGPS system.
<i>PRODUCT_START_YEAR</i> <i>PRODUCT_START_TIME</i>	The year/time limit for the earliest observation.
<i>PRODUCT_END_YEAR,</i> <i>PRODUCT_END_TIME</i>	The year/time limit for the latest observation.
<i>SW_VERSION</i>	The version of the RGPS software used to create this product.
<i>NW_LAT, NW_LONG,</i> <i>NE_LAT, NE_LONG,</i> <i>SW_LAT, SW_LONG,</i> <i>SE_LAT, SE_LONG</i>	The corner points of the initial datatake. The initial gridpoints are created within these bounds.

8.2.2 Ice Deformation: Area Change and Ice Motion Derivatives

The area change and ice motion spatial derivatives data contain multiple records. Each cell contains multiple observations of area change and ice motion spatial derivatives available up to the time of product creation. The records are in row order. Each record has the following format.

Field	Description
<i>CELL_ID</i>	Unique cell identifier assigned when the grid was created.
<i>BIRTH_YEAR,</i> <i>BIRTH_TIME</i>	The year/time of the creation of this cell.
<i>N_OBS</i>	The number of observations of this cell.
<i>OBS_YEAR_1,</i> <i>OBS_TIME_1</i>	The year/time of the first observation.
<i>X_MAP_1</i> <i>Y_MAP_1</i>	The map coordinates of the center of the cell.
<i>X_DISP_1,</i> <i>Y_DISP_1</i>	The displacement of the cell center between this and the last observation.
<i>C_AREA_1</i>	The cell area at the time of this observation.
<i>D_AREA_1</i>	The change in the cell area between this observation and the last

	observation.
<i>DTP 1</i>	The time interval between this and the last observation.
<i>DUDX 1,</i> <i>DUDY 1,</i> <i>DVDX 1,</i> <i>DVDY 1</i>	The derivatives as defined above.
.	
.	
.	
<i>OBS_YEAR N,</i> <i>OBS_TIME N</i>	The year/time of the <i>Nth</i> observation.
<i>X_MAP N,</i> <i>Y_MAP N</i>	The map coordinates of the center of the cell.
<i>X_DISP N,</i> <i>Y_DISP N</i>	The displacement of the cell center between this and the last observation.
<i>C_AREA N</i>	The cell area at the time of this observation.
<i>D_AREA N</i>	The change in the cell area between this observation (<i>N</i>) and the last observation (<i>N-1</i>).
<i>DTP N</i>	The time interval between this and the last observation.
<i>DUDX N,</i> <i>DUDY N,</i> <i>DVDX N,</i> <i>DVDY N</i>	The derivatives as defined above.

9. Area/Open Water Fraction (Product C)

9.1 Algorithm Description

The summer open water fraction within each cell is determined with an algorithm which uses the wind dependent backscatter characteristics of open water. We first compute the expected backscatter cross-section of open water using the surface wind speed and its direction relative to the radar look direction at each point. A C-HH model function (constructed from current C-VV model functions using the expected co-polarized response of open water) is used to provide the backscatter cross-section of open water. Summer ice (bare ice, ice with wet snow cover) has a very narrow range of backscatter, between -17dB and -12dB. At C-HH, depending on the wind velocity and incidence angle, the backscatter of open water could overlap, be above or below that of the ice. We anticipate that a refinement of this algorithm will be made based on the backscatter of open water at C-HH. Also, we do not estimate the open water fraction if the backscatter of water overlaps with that of ice. At points where the open water backscatter is above or below that of the ice, we use backscatter thresholds computed using the model function to determine whether a pixel belongs to the open water category.

9.2 Description (Product C) - Open Water Fraction

This product contains the open water fraction at each cell.

9.2.1 Open Water Fraction: Metadata Record

Field Name	Description
<i>PID</i>	RGPS product identifier (see section 4).
<i>PROD_DESCRIPTION</i>	Description of Product e.g. Lagrangian Ice Motion, Deformation, etc.
<i>N CELLS</i>	Number of cells contained in this product.
<i>CREATE_YEAR,</i> <i>CREATE_TIME</i>	The year/time this product was created by the RGPS system.
<i>SEASON_START_YEAR,</i> <i>SEASON_START_TIME</i>	The year/time limit for the earliest observation.
<i>SEASON_END_YEAR,</i> <i>SEASON_END_TIME</i>	The year/time limit for the latest observation.
<i>SW_VERSION</i>	The version of the RGPS software used to create this product.
<i>NW_LAT, NW_LONG,</i> <i>NE_LAT, NE_LONG,</i> <i>SW_LAT, SW_LONG,</i> <i>SE_LAT, SE_LONG</i>	The corner points of the initial datatake. The initial gridpoints are created within these bounds.

9.2.2 Open Water Fraction: Area/Open Water Fraction Data

The area/open water fraction data contain multiple records. Each record contains the area/open water fraction estimates for a cell. The records are in row order. Each record has the following format.

Field	Description
<i>CELL_ID</i>	Cell identifier.
<i>OBS_YEAR,</i> <i>OBS_TIME</i>	Year of observation.
<i>BIRTH_YEAR,</i> <i>BIRTH_TIME</i>	The year/time this cell was created.
<i>X_MAP,</i> <i>Y_MAP</i>	The center location of this cell.
<i>CELL_TEMP</i>	Temperature at cell center.
<i>MDD</i>	Cumulative melting degree days.
<i>I_AREA</i>	Initial cell area.
<i>C_AREA</i>	Current cell area.
<i>OW_FRAC</i>	Open water fraction.

10. Eulerian Ice Motion (Product E)

10.1 Description (Product E) - Eulerian Ice Motion

This product contains the results of ice motion derived from a pair of image frames.

10.1.1 Eulerian Ice Motion: Metadata Record

Field Name	Description
<i>PID</i>	RGPS product identifier (see section 4).
<i>PROD_DESCRIPTION</i>	Description of Product e.g. Lagrangian Ice Motion, Deformation etc.
<i>APID</i>	Image A Product identifier.
<i>BPID</i>	Image B Product identifier.
<i>ACENTYEAR</i> <i>ACENTTIME</i>	The scene year/time of image A.
<i>BCENTYEAR</i> <i>BCENTTIME</i>	The scene year/time of image B.
<i>A_TL_X, A_TL_Y</i> <i>A_TR_X, A_TR_Y</i> <i>A_BR_X, A_BR_Y</i> <i>A_BL_X, A_BL_Y</i>	The corner point locations of image A.
<i>B_TL_X, B_TL_Y</i> <i>B_TR_X, B_TR_Y</i> <i>B_BR_X, B_BR_Y</i> <i>B_BL_X, B_BL_Y</i>	The corner point locations of image B.
<i>PIXEL_SP</i>	Pixel spacing
<i>CREATE_YEAR</i> <i>CREATE_TIME</i>	The year/time this product was created by the RGPS system.
<i>GRID_W_OBS</i>	Grid elements with observations.
<i>NPIX_A,</i> <i>NREC_A</i>	Number of pixels across/down image A.
<i>NPIX_B,</i> <i>NREC_B</i>	Number of pixels across/down image B.
<i>AVG_DISP_X,</i> <i>AVG_DISP_Y</i>	Average displacement in x and y.
<i>D_TIME</i>	Time separation between images.
<i>GRIDSPACE</i>	Grid element spacing.
<i>SW_VERSION</i>	The version of the RGPS software used to create this product.
<i>ALGO_TYPE</i>	Algorithm type

10.1.2 Eulerian Ice motion: Motion Data

Field	Description
<i>A_GRID_X</i> , <i>A_GRID_Y</i>	Grid point location on image A.
<i>B_GRID_X</i> , <i>B_GRID_Y</i>	Grid point location on image B.
<i>DISP_X</i> , <i>DISP_Y</i>	Displacement of grid point.
<i>ROT_ANGLE</i>	Rotation Angle.
<i>Q_FLAG</i>	Quality flag (see Section 5).

11. Melt Onset /Freeze Up (Product F)

11.1 Algorithm Overview

The backscattering cross section of a Lagrangian cell is recorded at each time step. A time series of backscattering cross section histogram of each cell is used to determine the date of melt onset and freeze-up. The melt onset algorithm tracks the peak of the histogram for cells with more than 50% multiyear ice [Winebrenner et al., 1994, Winebrenner et al., 1996]. The detection criterion is when the peak value dips below a predetermined threshold. We estimate the date to be the time when the temporally interpolated peak crosses this threshold. The freeze-up algorithm also tracks the peak of the backscattering histogram. When this peak remains above a specified threshold for a period of N days, estimate M days prior to the threshold crossing to be the date of freeze.

11.2 Description (Product F) - Melt Onset/Freeze Up

This product contains the dates of melt onset or freeze up at each of the cells.

11.2.1 Melt Onset/Freeze Up: Metadata Record

Field Name	Description
<i>PID</i>	RGPS product identifier (see section 4).
<i>PROD_DESCRIPTION</i>	Description of Product e.g. Lagrangian Ice Motion, Deformation, etc.
<i>N_CELLS</i>	Number of cells contained in this product.
<i>CREATE_YEAR,</i> <i>CREATE_TIME</i>	The year/time this product was created by the RGPS system.
<i>SEASON_START_YEAR,</i> <i>SEASON_START_TIME</i>	The year/time limit for the earliest observation.
<i>SEASON_END_YEAR,</i> <i>SEASON_END_TIME</i>	The year/time limit for the latest observation.
<i>SW_VERSION</i>	The version of the RGPS software used to create this product.
<i>NW_LAT, NW_LONG,</i> <i>NE_LAT, NE_LONG,</i> <i>SW_LAT, SW_LONG,</i> <i>SE_LAT, SE_LONG</i>	The corner points of the initial datatake. The initial gridpoints are created within these bounds.

11.2.2 Melt Onset/Freeze Up: Dates

The dates are stored here.

Field Name	Description
<i>CELL_ID</i>	cell identifier
<i>TRANSITION_YEAR,</i> <i>TRANSITION_TIME</i>	Year/time of melt onset/freeze up.
<i>X_MAP,</i> <i>Y_MAP</i>	Center location of cell.

12. Gridded Wind/Temperature/Pressure Fields(Product M)

This product contains the daily geostrophic wind, air temperature and pressure fields on a 50 km SSM/I grid. The wind and pressure fields are re-gridded from fields provided by the International Arctic Buoy Program (IABP). The 2-m air temperatures are provided by the POLES project [Martin and Munoz, 1997].

12.1 Description (Product M) - Wind/Temperature/Pressure Fields

The gridded wind, temperature and pressure data are contained in the product.

12.1.1 Gridded Wind/Temperature/Pressure: Metadata Record

Field Name	Description
<i>PID</i>	RGPS product identifier (see section 4).
<i>PROD_DESCRIPTION</i>	Description of Product e.g. Lagrangian Ice Motion, Deformation etc.
<i>N_GRIDS</i>	Number of grid points used in the creation of this product.
<i>CREATE_YEAR,</i> <i>CREATE_TIME</i>	The year/time this product was created by the RGPS system.
<i>MET_YEAR/MET_TIME</i>	The year/time of the analysis.
<i>SW_VERSION</i>	The version of the RGPS software used to create this product.

12.1.2 Gridded Wind/Temperature/Pressure: Data

The meteorological data contain multiple records. Each record contains wind vector, pressure and temperature at each grid point. The records are in row order. Each record has the following format.

Field	Description
<i>X_MAP,</i> <i>Y_MAP</i>	Map location of grid points.
<i>U_WIND,</i> <i>V_WIND</i>	Geostrophic wind vector.
<i>PRESSURE</i>	Surface air pressure.
<i>TEMP</i>	2-m air temperature.

13. References

- Coon, M. D., G. S. Knoke and D. C. Echert, Compensating for daily lead-width motion when calculating open-water production from weekly data. NWRA Report. NWRA-CR-96-R158.
- DMSP SSM/I Brightness Temperature Sea Ice Concentration Grids for the Polar Regions, User's Guide, NSIDC, 1996.
- Fowler, C., W. Emery and J. Maslanik, The Consequences of 7-day Sampling for RADARSAT Ice Motions and Derived Fields, NSIDC report, 1996.
- Hopkins, M. A., J. Tuhkuri and M. Lensu, Rafting and ridging of ice sheets, *J. Geophys. Res.*, 104 (C6), 13605-13613, 1999.
- Kwok, R. and T. Baltzer, The Geophysical Processor System at the Alaska SAR Facility. *Photogramm. Engrg. and Remote Sens.*, Vol. 61, No. 12, 1445-1453, 1995.
- Kwok, R., D. A. Rothrock, H. L. Stern and G. F. Cunningham, Determination of Ice Age using Lagrangian Observations of Ice Motion, *IEEE Trans. Geosci. Remote Sens.*, Vol. 33, No. 2, pp. 392-400, 1995.
- Kwok, R. and G. Cunningham, Backscatter Characteristics of The Sea Ice Cover in the Winter Beaufort Sea, *J. Geophys. Res.*, 99 (C4), 7787-7802, 1994.
- Kwok, R., E. Rignot, B. Holt and R. G. Onstott, Identification of Sea Ice Types in Spaceborne SAR Data, *J. Geophys. Res.*, 97 (C2), 2391-2402, 1992.
- Kwok, R., J.C. Curlander, R. McConnell and S. Pang, An Ice Motion Tracking System at the Alaska SAR Facility, *IEEE J. of Oceanic Engineering*, Vol. 15, No. 1, 44-54, 1990.
- Martin, S. and E. A. Munoz, Properties of the Arctic 2-m air temperature for 1979-present derived from a new gridded data set, *J. Climate*, 10, 1428-1440, 1997.
- Maykut, G. A., The Surface Heat and Mass Balance, in *Geophysics of Sea Ice*, Ed. N. Untersteiner, Series B: Physics Vol. 146, Plenum Press, 1986, p. 423.
- Parmeter, R. R. and M. Coon, Model of pressure ridge formation in sea ice, *J. Geophys. Res.*, 77, 6565-6575, 1972.
- Raney, R. K., A. P. Luscombe, E. J. Langham and S. Ahmed, RADARSAT, *Proceedings of the IEEE*, Vol.79, No. 6, pp 839-849, 1991.

Winebrenner, D. P., E. D. Nelson, R. Colony, R. D. West, Observations of melt onset on multiyear Arctic sea ice using ERS 1 synthetic aperture radar, *J. Geophys. Res.*, 99(C11), pp. 22425-22441, 1994.

Winebrenner, D. P., B. Holt, E. D. Nelson, Observation of autumn freeze-up in the Beaufort and Chukchi Seas using ERS-1 synthetic aperture radar, *J. Geophys. Res.*, 101(C7), 16401-16419, 1996.